

Fig. S1. Western blot analysis of Sra in *APP*-expressing flies. Western blot analysis with an anti-Sra antibody shows that Sra protein is not altered in pan-neuronally *APP*-expressing (*elav>APP*) fly heads compared with that of the control (*elav-GAL4* and *UAS-APP*). Actin was used as an internal loading control. All data are expressed as mean \pm s.e. (Tukey-Kramer test, $n = 4$, NS, not significant).

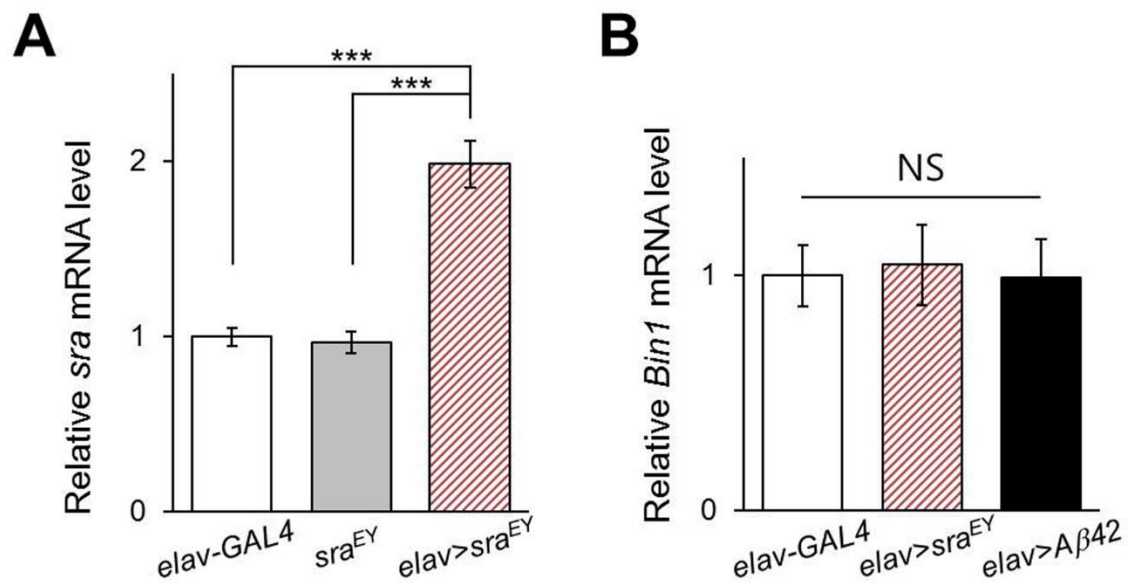


Fig. S2. Analyses of *sra* and *Bin1* gene expression in adult fly heads using real-time quantitative PCR. (A) Real-time quantitative PCR results show relative fold change in *sra* (A) and *Bin1* (B) transcript levels for the indicated fly lines. All data are expressed as mean \pm s.e. (A, Tukey-Kramer test, $n \geq 4$, *** $p < 0.001$; B, Tukey-Kramer test, $n \geq 10$; NS, not significant).

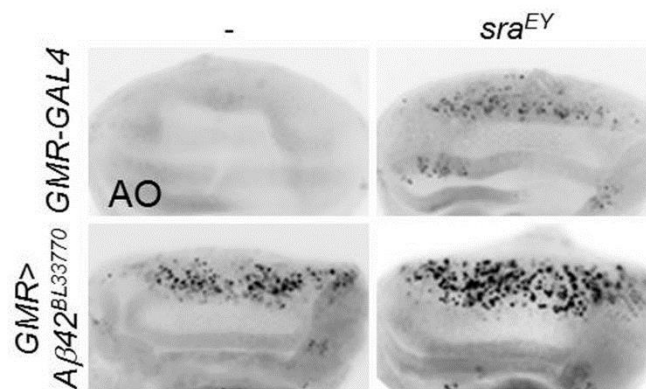


Fig. S3. Overexpression of *sra* aggravates *Aβ42*-induced cell death in the *Drosophila* larval eye disc. Representative images of AO-stained *sra*- and *Aβ42*-expressing larval eye imaginal discs (n = 10). AO, acridine orange.

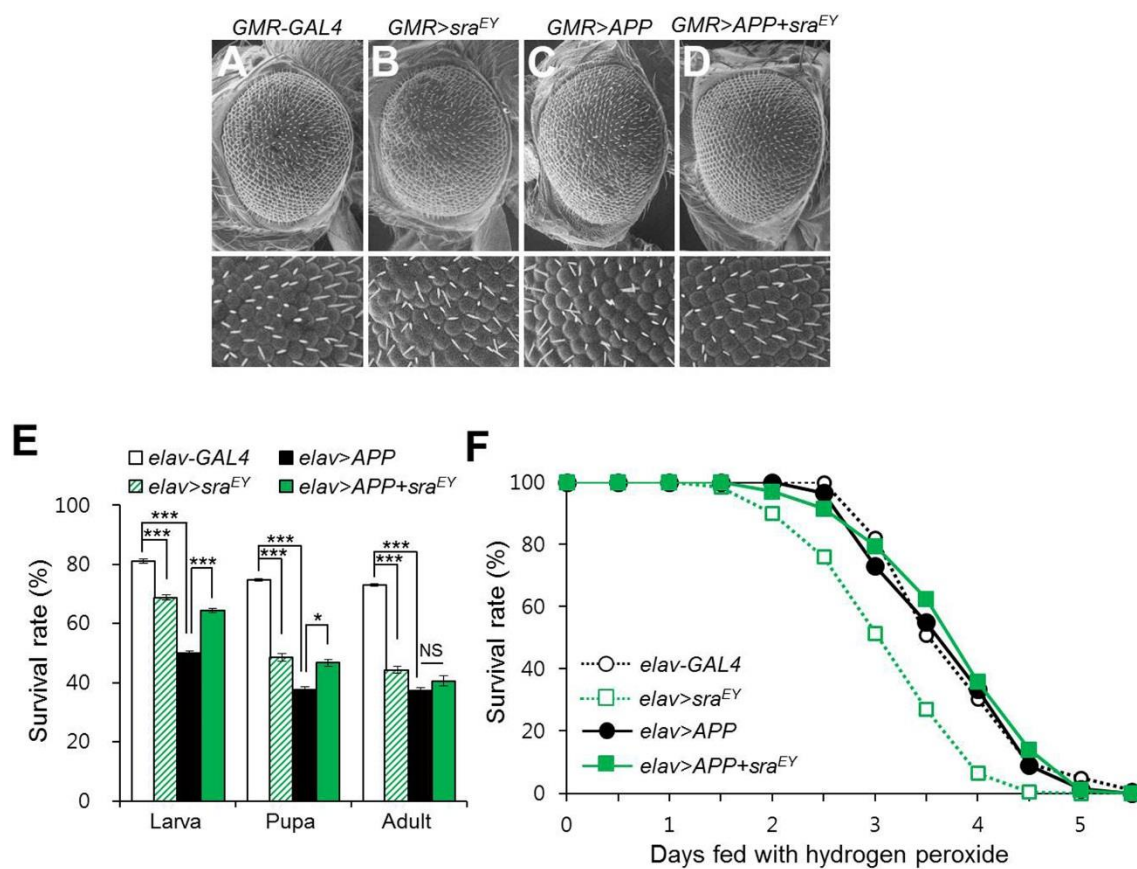


Fig. S4. Overexpression of *sra* partially rescues *APP*-expressing fly phenotypes. (A-D) Eye phenotypes induced by ectopic expression of *APP* in the developing eye were partially rescued by *sra* overexpression. The *APP*-expressing adults exhibit a mild rough eye phenotype (C) relative to that of the control eye (A). Overexpression of *sra* alone resulted in a marginally rough eye phenotype (B) when compared to that of the control (A). Overexpression of *sra* in *APP*-expressing flies rescued the rough eye phenotype (D) relative to that of *APP*-expressing flies (C). The lower pictures are the magnified images of the each genotype in the upper pictures. (E) Survival rates of pan-neuronal *APP*-expressing flies with *sra* overexpression (*elav>APP+sra^{EY}*). The effects of overexpressed *sra* (*elav>sra^{EY}*) in the

control (*elav-GAL4*) are also shown (Tukey-Kramer test, $n \geq 400$, $*p < 0.05$, $***p < 0.001$, NS, not significant). (F) Survival rates of *APP*-expressing flies overexpressing *sra* under oxidative stress conditions ($n = 200$). The Kaplan-Meier estimator and log-rank test was used to determine significant differences in survival rates of samples. *elav-GAL4* vs *elav>sra^{EY}*: $p < 0.0001$; *elav-GAL4* vs *elav>APP*: $p = 0.5813$; *elav>sra^{EY}* vs *elav>APP+sra^{EY}*: $p < 0.0001$; *elav>APP* vs *elav>APP+sra^{EY}*: $p = 0.2268$.

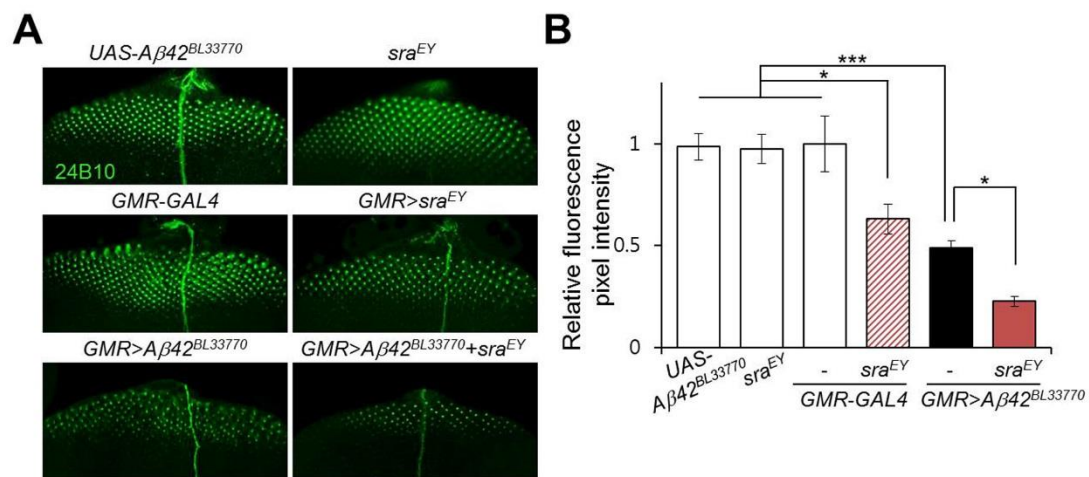


Fig. S5. Overexpression of *sra* aggravates *Aβ42*-induced phenotypes in *Aβ42*-expressing flies.

(A) Representative immunohistochemistry images of photoreceptor neurons in larval eye discs. Each indicated fly was stained with an anti-Chaoptin antibody (24B10) to show photoreceptor neurons. Magnification of the pictures, $\times 200$. (B) The graph shows the relative fluorescence pixel intensity in photoreceptor neurons (Tukey-Kramer test, $n \geq 10$, $*p < 0.05$, $***p < 0.001$, NS, not significant).

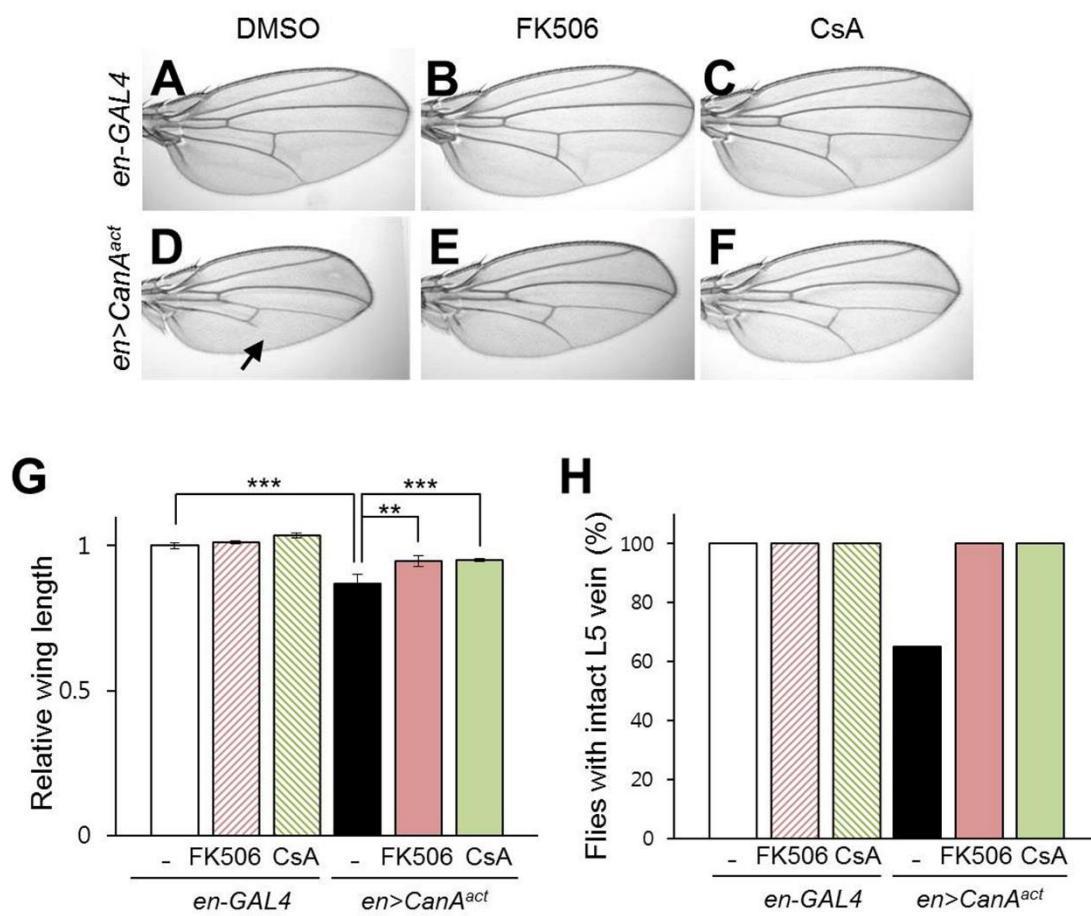


Fig. S6. Chemical calcineurin inhibitors inhibit calcineurin signaling. FK506 and CsA, chemical calcineurin inhibitors, suppress the phenotypes induced by a constitutively active form of calcineurin (*CanA^{act}*). (A-F) Representative images of developing wing phenotypes in DMSO-fed (A, D), 50 μ M FK506-fed (B, E), and 20 μ M CsA-fed (C, F) flies with (D-F; *en>CanA^{act}*) or without (A-C; *en-GAL4*) *CanA^{act}* expression. The reduced wing size and loss of wing veins (arrow) resulting from *CanA^{act}* expression were suppressed by the inhibitors. (G, H) The graph shows the relative size (G, all data are expressed as mean \pm s.e., Tukey-Kramer test, $n = 20$, ** $p < 0.01$, *** $p < 0.001$) and intact L5 vein (H, $n = 20$) in the developing wing in each experimental group. CsA, cyclosporin A.

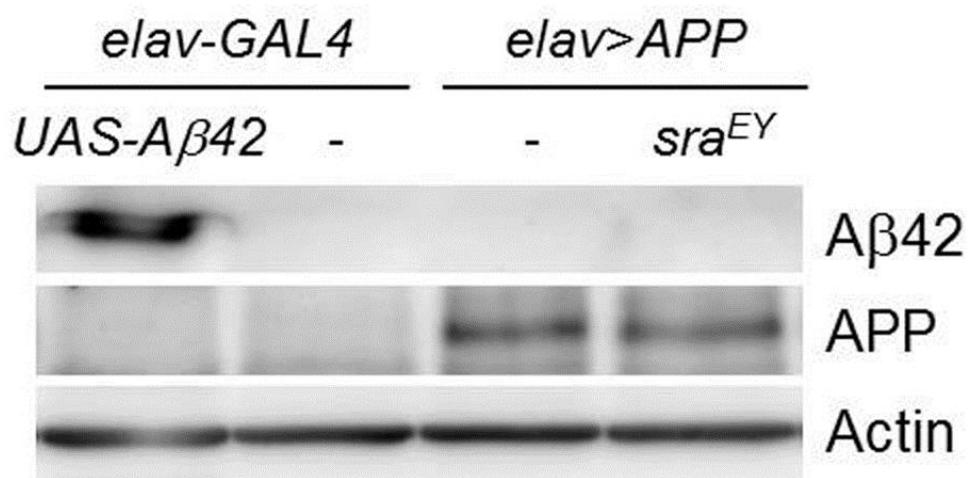


Fig. S7. Western blot analysis of Aβ42 levels in the head region of *Aβ42*- or *APP*-expressing flies. Aβ42 protein is not produced in *APP*-expressing (*elav>APP*) fly heads. The head extract of *Aβ42*-expressing flies (*elav>Aβ42*) was used as a positive control. Actin was used as an internal loading control.

Table S1. The genotypes of samples in figures.

No. figure	Symbol	Genotype
Fig. 1		
A-D	<i>sra</i> > <i>EGFP</i>	<i>UAS-2×EGFP/+; sra-GAL4/+</i>
	<i>sra</i> ^{KO}	<i>sra</i> ^{KO} / <i>sra</i> ^{KO}
E, F	<i>elav-GAL4</i>	<i>elav-GAL4/elav-GAL4</i>
	<i>UAS-Aβ42</i>	<i>UAS-Aβ42/UAS-Aβ42</i>
	<i>elav>Aβ42</i>	<i>UAS-Aβ42/UAS-Aβ42; elav-GAL4/elav-GAL4</i>
Fig. 2		
A-P	<i>sra</i> ^{EY}	<i>sra</i> ^{EY07182/+}
	<i>UAS-sra</i>	<i>UAS-sra/+</i>
	<i>GMR>sra</i> ^{EY}	<i>GMR-GAL4/+; sra</i> ^{EY07182/+}
	<i>GMR>sra</i>	<i>GMR-GAL4/UAS-sra</i>
	<i>GMR; sra</i> ^{KO/+}	<i>GMR-GAL4/+; sra</i> ^{KO/+}
	<i>GMR>DIAP1</i>	<i>GMR-GAL4/+; UAS-DIAP1/+</i>
	<i>GMR-GAL4</i>	<i>GMR-GAL4/+</i>
	<i>GMR>Aβ42</i> ^{BL33770}	<i>GMR-GAL4, UAS-Aβ42</i> ^{BL33770/+}
	<i>GMR>Aβ42</i> ^{BL33770/+sra^{EY}}	<i>GMR-GAL4, UAS-Aβ42</i> ^{BL33770/+} ; <i>sra</i> ^{EY07182/+}
	<i>GMR>Aβ42</i> ^{BL33770/+sra}	<i>GMR-GAL4, UAS-Aβ42</i> ^{BL33770/+} / <i>UAS-sra</i>
	<i>GMR>Aβ42</i> ^{BL33770/+sra^{KO/+}}	<i>GMR-GAL4, UAS-Aβ42</i> ^{BL33770/+} ; <i>sra</i> ^{KO/+}
	<i>GMR>sra</i> ^{EY} + <i>DIAP1</i>	<i>GMR-GAL4/+; sra</i> ^{EY07182/+} / <i>UAS-DIAP1</i>
Q, S, T	<i>elav-GAL4</i>	<i>elav-GAL4/elav-GAL4</i>
	<i>elav>Aβ42</i>	<i>UAS-Aβ42/UAS-Aβ42; elav-GAL4/elav-GAL4</i>
	<i>elav>sra</i> ^{EY}	<i>elav-GAL4, sra</i> ^{EY07182/+} / <i>elav-GAL4, sra</i> ^{EY07182/+}
	<i>elav>Aβ42+sra</i> ^{EY}	<i>UAS-Aβ42/UAS-Aβ42; elav-GAL4, sra</i> ^{EY07182/+} / <i>elav-GAL4, sra</i> ^{EY07182/+}
R	<i>elav-GAL4</i>	<i>elav-GAL4/+</i>
	<i>sra</i> ^{EY}	<i>sra</i> ^{EY07182/+}
	<i>UAS-Aβ42</i>	<i>UAS-Aβ42/+</i>
	<i>elav>Aβ42</i>	<i>UAS-Aβ42/+; elav-GAL4/+</i>
	<i>elav>sra</i> ^{EY}	<i>elav-GAL4/sra</i> ^{EY07182/+}

	<i>elav>Aβ42+sra^{EY}</i>	<i>UAS-Aβ42/+; elav-GAL4/sra^{EY07182}</i>
Fig. 3		
A-B	<i>UAS-Aβ42</i>	<i>UAS-Aβ42/UAS-Aβ42</i>
	<i>sra^{EY}</i>	<i>sra^{EY07182}/sra^{EY07182}</i>
	<i>elav-GAL4</i>	<i>elav-GAL4/elav-GAL4</i>
	<i>elav>sra^{EY}</i>	<i>elav-GAL4, sra^{EY07182}/elav-GAL4, sra^{EY07182}</i>
	<i>elav>Aβ42</i>	<i>UAS-Aβ42/UAS-Aβ42; elav-GAL4/elav-GAL4</i>
	<i>elav>Aβ42+sra^{EY}</i>	<i>UAS-Aβ42/UAS-Aβ42; elav-GAL4, sra^{EY07182}/elav-GAL4, sra^{EY07182}</i>
C	<i>GMR-GAL4</i>	<i>GMR-GAL4/GMR-GAL4</i>
	<i>GMR>sra^{EY}</i>	<i>GMR-GAL4/GMR-GAL4; sra^{EY07182}/sra^{EY07182}</i>
	<i>GMR>Aβ42^{BL33770}</i>	<i>GMR-GAL4, UAS-Aβ42^{BL33770}/GMR-GAL4, UAS-Aβ42^{BL33770}</i>
	<i>GMR>Aβ42^{BL33770}+sra^{EY}</i>	<i>GMR-GAL4, UAS-Aβ42^{BL33770}/GMR-GAL4, UAS-Aβ42^{BL33770}; sra^{EY07182}/sra^{EY07182}</i>

	<i>sra^{EY}</i>	<i>sra^{EY07182}/+</i>
Fig. 4		
	<i>UAS-Aβ42</i>	<i>UAS-Aβ42/+</i>
	<i>sra^{EY}</i>	<i>sra^{EY07182}/+</i>
	<i>elav-GAL4</i>	<i>elav-GAL4/+</i>
	<i>sra^{EY}</i>	<i>sra^{EY07182}/+</i>
	<i>elav>Aβ42+sra^{EY}</i>	<i>UAS-Aβ42/+; elav-GAL4/sra^{EY07182}</i>

	<i>elav-GAL4</i>	<i>elav-GAL4/+</i>
Fig. 5		
	<i>elav>sra^{EY}</i>	<i>elav-GAL4/sra^{EY07182}</i>
	<i>elav>Aβ42</i>	<i>UAS-Aβ42/+; elav-GAL4/+</i>
	<i>elav>Aβ42+sra^{EY}</i>	<i>UAS-Aβ42/+; elav-GAL4/sra^{EY07182}</i>

	<i>GMR-GAL4</i>	<i>GMR-GAL4/+</i>
Fig. 6		
A-K	<i>GMR>CanAi</i>	<i>GMR-GAL4/+; UAS-CanA1 RNAi/+</i>
	<i>GMR>CanBi</i>	<i>GMR-GAL4/+; UAS-CanB RNAi/+</i>
	<i>GMR>Aβ42^{BL33770}</i>	<i>GMR-GAL4, UAS-Aβ42^{BL33770}/+</i>
	<i>GMR>Aβ42^{BL33770}+CanAi</i>	<i>GMR-GAL4, UAS-Aβ42^{BL33770}/+; UAS-CanA1 RNAi/+</i>
	<i>GMR>Aβ42^{BL33770}+CanBi</i>	<i>GMR-GAL4, UAS-Aβ42^{BL33770}/+; UAS-CanB RNAi/+</i>
	<i>CanAi</i>	<i>UAS-CanA1 RNAi/+</i>

L, M	<i>elav-GAL4</i>	<i>elav-GAL4/+</i>
	<i>elav>CanAi1</i>	<i>elav-GAL4/UAS-CanAi1 RNAi</i>
	<i>elav>Aβ42</i>	<i>UAS-Aβ42/+; elav-GAL4/+</i>
	<i>elav>Aβ42+CanAi1</i>	<i>UAS-Aβ42/+; elav-GAL4/UAS-CanAi1 RNAi</i>

Fig. S1

	<i>elav-GAL4</i>	<i>elav-GAL4/+</i>
	<i>UAS-APP</i>	<i>UAS-APP-N-myc/+</i>
	<i>elav>APP</i>	<i>UAS-APP-N-myc/+; elav-GAL4/+</i>

Fig. S2

	<i>elav-GAL4</i>	<i>elav-GAL4/+</i>
	<i>sra^{EY}</i>	<i>sra^{EY07182}/+</i>
	<i>elav>sra^{EY}</i>	<i>elav-GAL4/sra^{EY07182}</i>
	<i>elav>Aβ42</i>	<i>UAS-Aβ42/+; elav-GAL4/+</i>

Fig. S3

	<i>GMR-GAL4</i>	<i>GMR-GAL4/GMR-GAL4</i>
	<i>GMR>sra^{EY}</i>	<i>GMR-GAL4/GMR-GAL4; sra^{EY07182}/sra^{EY07182}</i>
	<i>GMR>Aβ42^{BL33770}</i>	<i>GMR-GAL4, UAS-Aβ42^{BL33770}/GMR-GAL4, UAS-Aβ42^{BL33770}</i>
	<i>GMR>Aβ42^{BL33770}+sra^{EY}</i>	<i>GMR-GAL4, UAS-Aβ42^{BL33770}/GMR-GAL4, UAS-Aβ42^{BL33770}; sra^{EY07182}/sra^{EY07182}</i>

Fig. S4

A-D	<i>GMR-GAL4</i>	<i>GMR-GAL4/+</i>
	<i>GMR>sra^{EY}</i>	<i>GMR-GAL4/+; sra^{EY07182}/+</i>
	<i>GMR>APP</i>	<i>GMR-GAL4/UAS-APP-N-myc</i>
	<i>GMR>APP+sra^{EY}</i>	<i>GMR-GAL4/UAS-APP-N-myc; sra^{EY07182}/+</i>
E, F	<i>elav-GAL4</i>	<i>elav-GAL4/+</i>
	<i>elav>sra^{EY}</i>	<i>elav-GAL4/sra^{EY07182}</i>
	<i>elav>APP</i>	<i>UAS-APP-N-myc/+; elav-GAL4/+</i>
	<i>elav>APP+sra^{EY}</i>	<i>UAS-APP-N-myc/+; elav-GAL4/ sra^{EY07182}</i>

Fig. S5

	<i>UAS-Aβ42^{BL33770}</i>	<i>UAS-Aβ42^{BL33770}/UAS-Aβ42^{BL33770}</i>
	<i>sra^{EY}</i>	<i>sra^{EY07182}/sra^{EY07182}</i>
	<i>GMR-GAL4</i>	<i>GMR-GAL4/GMR-GAL4</i>
	<i>GMR>sra^{EY}</i>	<i>GMR-GAL4/GMR-GAL4; sra^{EY07182}/sra^{EY07182}</i>

<i>GMR>Aβ42^{BL33770}</i>	<i>GMR-GAL4, UAS-Aβ42^{BL33770}/GMR-GAL4, UAS-Aβ42^{BL33770}</i>
<i>GMR>Aβ42^{BL33770}+sra^{EY}</i>	<i>GMR-GAL4, UAS-Aβ42^{BL33770}/GMR-GAL4, UAS-Aβ42^{BL33770}; sra^{EY07182}/sra^{EY07182}</i>

Fig. S6

<i>en-GAL4</i>	<i>en2.4-GAL4/+</i>
<i>en>CanA^{act}</i>	<i>en2.4-GAL4/UAS-CanA^{act}</i>

Fig. S7

<i>elav>Aβ42</i>	<i>UAS-Aβ42/+; elav-GAL4/+</i>
<i>elav-GAL4</i>	<i>elav-GAL4/+</i>
<i>elav>APP</i>	<i>UAS-APP-N-myc/+; elav-GAL4/+</i>
<i>elav>APP+sra^{EY}</i>	<i>UAS-APP-N-myc/+; elav-GAL4/sra^{EY07182}</i>